World Academy of Science, Engineering and Technology
International Journal of Civil and Environmental Engineering
Vol:16, No:6, 2022

Numerical Evaluation of Turbulent Friction on Walls in the Penstock of the Trois-Gorges Dam by the Swamee-Jain Method

T. Tchawe Moukam, N. Ngongang François, D. Thomas, K. Bienvenu, T. -Toko Dénis

***Abstract*—**Since the expression of the coefficient of friction by Colebrook-White which turns out to be an implicit equation, equations have been developed to facilitate their applicability. In this work, this equation was applied to the penstock of the Three Gorges dam in order to observe the evolution of the turbulent boundary layer and the friction along the walls. Thus, the study is being carried out using a 3D digital approach in FLUENT in order to take into account the wall effects. It appears that according to the position of the portions, we have a variation in the evolutions of the turbulent friction and of the values of the boundary layer. We also observe that the inclination of the pipe has a significant influence on this turbulent friction; similarly, one could not make a fair evaluation of the latter without specifying the choice and location of the wall.

***Keywords*—**Hydroelectric dam, penstock, turbulent friction, boundary layer, CFD.

I. Introduction

IN a hydroelectric power station, the penstock is the pipe that connects the water reservoir (retaining dam) to the turbine that drives the electric generator. In this pipe, strong pressures (that can cause very great material damage) are exerted on the walls.

Penstock pipes are the site of very large pressure drops of up to 15% caused by friction [1]. After the implicit Colebrook-White expression [2], [3] for the determination of the coefficient of friction, several other authors have developed this expression in order to make it explicit. The formula of Swamee and Jain of 1976 [4] is the formula most used today [5]. It constitutes an approximate solution to the Colebrook-White equation. This formula is a constant and only takes into account the Reynolds number of the inlet flow and the relative roughness of the pipe.

We evaluate in this document from the Swamee and Jain formula, the coefficient of turbulent friction in the penstock of the Three Gorges dam. Its diameter is 12.4 m and it is made up of three portions. We will highlight the values (heights) of the turbulent boundary layers in the penstock for different speeds and on different walls, at the same time observing the impact of the geographical arrangement of the penstocks.

II. Material and Methods

The Three Gorges hydroelectric dam is the largest dam in the world, with penstocks 12.4 m in diameter [6]. Its model and accompanying boundary conditions are given by Fig. 1. Its penstock is made up of three sections. The first portion goes from the water hold to the first elbow, the second portion is between the two elbows, and the third portion goes between the second elbow and the turbine inlet.

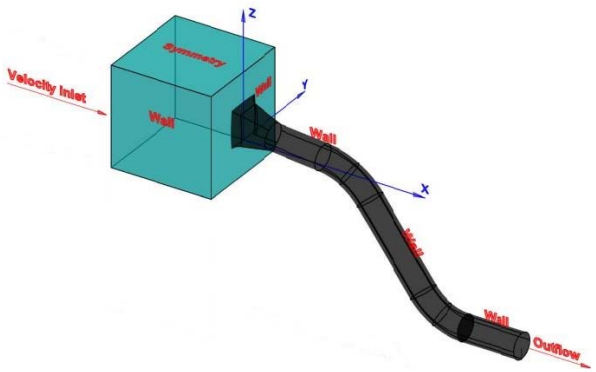

Fig. 1 (a) Model of the study area with boundary conditions

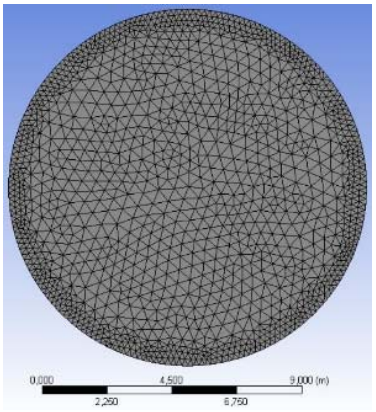

Fig. 1 (b) Mesh structure: cross section (present study)

Tchawe Tchawe Moukam is with the Department of Mechanical Engineering of the ENSAI, University of Ngaoundere, CO 455 Ngaoundere-Cameroon (corresponding author, phone: (+237) 674-768-612; e-mail: christophetchawe88@gmail.com).

F. N. Nkontchou is with the Department of Mechanical Engineering of the ENSAI, University of Ngaoundere, CO 455 Ngaoundere-Cameroon (e-mail: francis.nkontchou@gmail.com).

T. Djiako is with the Department of Mechanical Engineering and Energy of the ISTA, University Institute of the Gulf of Guinea, CO 12489 Douala-Cameroon (e-mail: thomasdjako@yahoo.fr).

B. Kenmeugne is with the Department of Mechanical Engineering of the ENSPY, University of Yaounde 1, CO 8390 Yaounde-Cameroon (e-mail: kenmeugneb@gmail.com).

D. Tcheukam-Toko is with the Department of Mechanical Engineering of the COT, University of Buea, CO 63 Buea-Cameroon (e-mail: tcheukam_toko@yahoo.fr).

In this work, k-ε Realisable is used as a turbulence model because it is well suited for flows with high curvature, boundary layers having strong opposing pressure gradient and vortices. It is considered isotropic. The SIMPLEC velocity-pressure coupling method is used to solve the second order equations, with a convergence criterion of 10^{-6} [7]. Our study is essentially based on the phenomena occurring near the walls. We made a third degree smoothing close to the walls to reduce calculation errors and the cells are regular tetrahedral. The approaching flow is stationary. The turbulence is isotropic. The discretization scheme is Body Force Weighted, and the near walls function considered is the standard wall function.

A. General Equation of the Problem

The equations that govern turbulent hydrodynamic flows are the laws of conservation of mass, momentum and energy. The flow in our case is considered to be isothermal. The flow has constant viscosity and is incompressible. It can be described by the velocity and pressure field governed by the Navier-Stokes equations [8], [9] cited by [10] and [11]. The fluid is assumed to be a Newtonian fluid. Therefore,

$$\frac{\partial U_i}{\partial U_j} = 0 \tag{1}$$

The dynamic conservation is:

$$\frac{\partial U_i}{\partial t} + \frac{\partial (U_j U_i)}{\partial x_j} = \frac{1}{\rho}\left(-\frac{\partial p}{\partial x_i} + \frac{\partial \tau_{ij}}{\partial x_i}\right) \tag{2}$$

where ρ the constant density, $\mathbf{p}$ is the static pressure load, $\boldsymbol{U_i}$ represents the velocities in $\boldsymbol{x_i}$ coordinate directions and $\boldsymbol{\tau_{ij}}$ the viscous stress tensor. For a Newtonian fluid [12]:

$$\tau_{ij} = \mu\left(\frac{\partial U_i}{\partial x_j} + \frac{\partial U_j}{\partial x_i}\right) \tag{3}$$

The variations within the flow are too rapid to be described in time and space. Also, the velocity details are lost. We adopt for the pressure and the velocity the following decomposition [12] cited by [7]:

$$u_i = \overline{u_\iota} + u_i' \tag{4}$$

with $\overline{u_\iota}$ and u_i' the average components of the fluctuating velocity ($i = 1, 2, 3$). The pressure and the other scalar values are as in [12] cited by [7] and [11]:

$$\phi = \bar{\phi} + \phi' \tag{5}$$

where ϕ a scalar such as pressure, energy, or other concentration.

We obtain the mean momentum equations by substituting expressions of this form for the flow variables in the continuity and instantaneous momentum equations while taking a time average. They can be written in the form of the Cartesian tensor [12] cited by [7]:

$$\frac{\partial \rho}{\partial t} + \frac{\partial}{\partial x_i}(\rho u_i) = 0 \tag{6}$$

$$\frac{\partial}{\partial t}(\rho u_i) + \frac{\partial}{\partial x_i}(\rho u_i u_j) = -\frac{\partial p}{\partial x_i} + \frac{\partial}{\partial x_j}\left[\mu\left(\frac{\partial u_i}{\partial x_j} + \frac{\partial u_j}{\partial x_i} + \frac{2}{3}\delta_{ij}\frac{\partial u_i}{\partial x_l}\right)\right] + \frac{\partial}{\partial x_j}\left(-\rho\overline{u_i' u_j'}\right) \tag{7}$$

We subsequently have additional terms that appear to represent the effects of turbulence. Thus the Reynolds stress $\rho\overline{u_i' u_j'}$, must be modeled to close (7) as used [12] cited by [7]; which allows us to use for closure equation the Boussinesq approximation [13]:

$$-\rho\overline{u_i' u_j'} = \mu\left(\frac{\partial u_i}{\partial x_j} + \frac{\partial u_j}{\partial x_i}\right) - \frac{2}{3}\left(\rho k + \mu_t \frac{\partial u_i}{\partial x_i}\right)\delta_{ij} \tag{8}$$

The transport equations for k and ε have as model:

$$\frac{\partial}{\partial t}(\rho k) + \frac{\partial}{\partial x_i}(\rho k U_j) = \frac{\partial}{\partial x_i}\left[\left(\mu + \frac{\mu_t}{\sigma_k}\right)\frac{\partial k}{\partial x_j}\right] + G_k + G_b + \rho\varepsilon + Y_M + S_k \tag{9a}$$

$$\frac{\partial}{\partial t}(\rho\varepsilon) + \frac{\partial}{\partial x_j}(\rho\varepsilon U_j) = \frac{\partial}{\partial x_j}\left[\left(\mu + \frac{\mu_t}{\sigma_\varepsilon}\right)\frac{\partial \varepsilon}{\partial x_j}\right] + \rho C_1 S_\varepsilon + \rho C_2 \frac{\varepsilon^2}{k + \sqrt{\nu\varepsilon}} + C_{1\varepsilon}\frac{\varepsilon}{k} C_{3\varepsilon} G_b + S_\varepsilon \tag{9b}$$

where $C_1 = \max\left[0{,}43\frac{\eta}{\eta+5}\right]$; $\eta = S_\varepsilon^k$; $C_{3\varepsilon} = \tanh\left[\frac{v}{u}\right]$ and describes the degree of influence of volume forces, $\boldsymbol{v}$ the component of the flow velocity parallel to the gravitational vector, and $\boldsymbol{u}$ the component of the flow velocity perpendicular to the gravitational vector.

$G_k = -\rho\overline{u_i' u_j'}\frac{\partial u_j}{\partial x_i}$

in (9a) is the generator term of the kinetic energy of turbulence due to the mean of the calculated velocity gradient. $G_b = \beta g_i \frac{\mu_t}{P_{rt}}\frac{\partial T}{\partial x_i}$ is equally, the generator term of the kinetic energy of turbulence due to the volume forces is. Y_M in (9a) is the fluctuation of the expansion in compressible turbulence, while C_1 and C_2 are their constants. For the turbulent Prandtl numbers for k and ε respectively, we have σ_k et σ_ε. Finally, user-defined terms are S_k and S_ε [12] cited by [7].

The turbulent viscosity is given by:

$$\mu_t = \rho C_\mu \frac{k^2}{\varepsilon} \tag{10}$$

C_μ is given by:

$$C_\mu = \frac{1}{A_0 + A_S\frac{kU^*}{\varepsilon}} \tag{11}$$

The constants are given by:

$$A_0 = 4{,}04;\ A_S = \sqrt{6}cos\phi$$
$$C_{1\varepsilon} = 1{,}44;\ C_2 = 1{,}9;\ \sigma_k 1{,}0;\ \sigma_\varepsilon = 1{,}2$$

B. Friction Coefficient Equation

The Swamee and Jain formula [4] is the relation used to

calculate the coefficient of friction ***f*** which is expressed by:

$$f = 0{,}25 \log\left(\frac{\varepsilon}{3{,}7D} + \frac{5{,}74}{0{,}9R_e}\right)^{-2} \quad (12)$$

N.B.: Solving these equations was made in FLUENT [14].

III. Results and Discussion

The evolution of friction will be presented on the bottom, top and side walls as a function of the Reynolds number, and for each of the three sections constituting our penstock. The speeds used depending on the water levels in the upstream reservoir are 7 m/s, 8 m/s and 9 m/s. This is based on the variation of the water level as a function of the period of the year in question [15]. The height interval considered for the calculation of the coefficient of friction in the three sections and on the three walls varies from 0.05 mm to 1000 mm. The results obtained are as follows:

A. Bottom Wall

Fig. 2 gives us the evolution of the value of f_{max} on the bottom wall for the three portions as a function of the thickness.

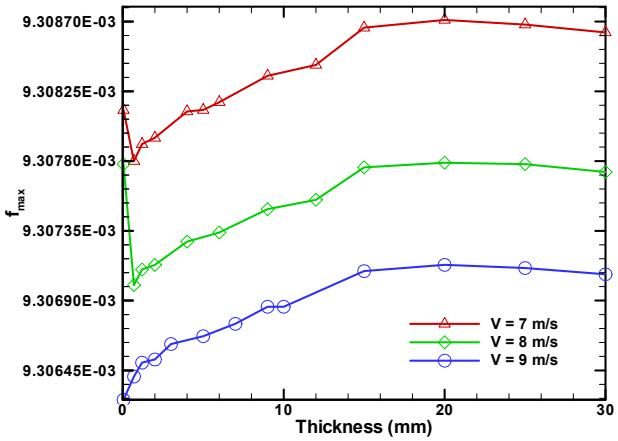

Fig. 2 (a) Evolution of the maximum friction on the bottom wall in the portion 1

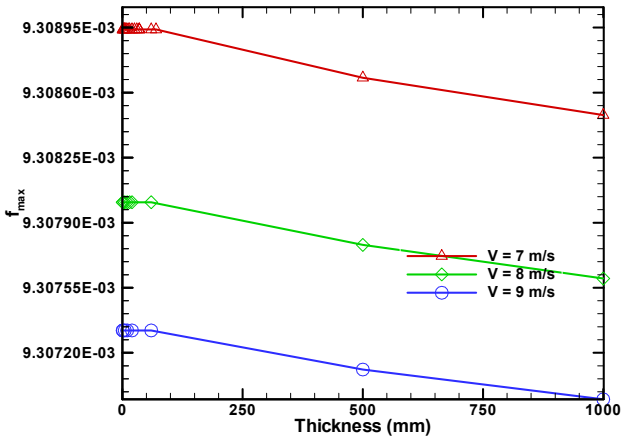

Fig. 2 (b) Evolution of the maximum friction on the bottom wall in the portion 2

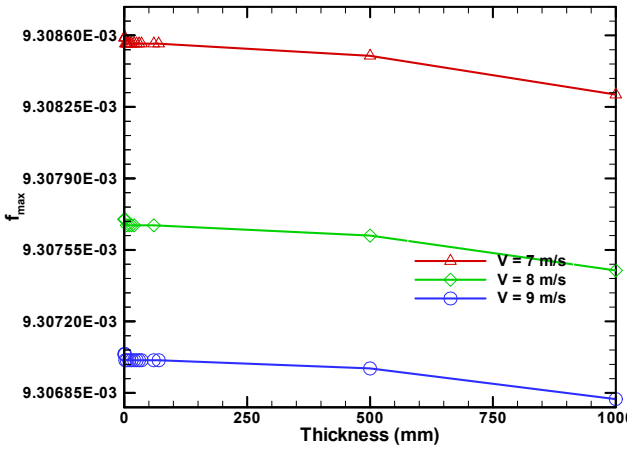

Fig. 2 (c) Evolution of the maximum friction on the bottom wall in the portion 3

The purpose of Figs. 2 (a)-(c) is to verify the quality of the results obtained from the data in the literature. Thus, we clearly observe that this coefficient is maximum near the walls; which therefore allows us to assess the applicability of this formula. We also see the constant evolution of turbulent friction with the fall of the Reynolds number. Likewise, it is difficult for us to predict exactly from this scale the height of the turbulent boundary layer. It will therefore be a question for us subsequently of reducing the scale in order to better assess this friction. Therefore, in the remainder of this document, we will reduce the study interval from 0.05 mm to a maximum of 30 mm for all study profiles.

Figs. 3 (a)-(c) give us the evolution of the value of f_{max} on the bottom wall for the three portions as a function of the thickness, for the range of 0.05 mm to 30 mm.

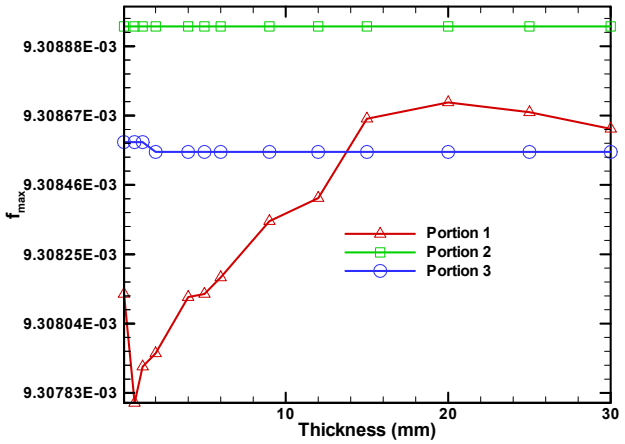

Fig. 3 (a) Evolution of the maximum friction on the bottom wall for v = 7 m/s

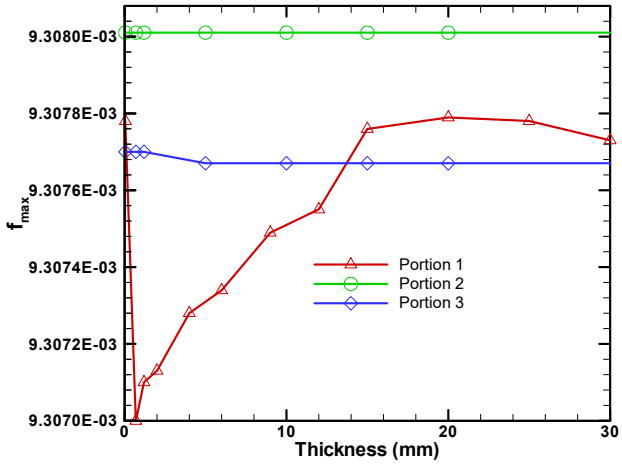

Fig. 3 (b) Evolution of the maximum friction on the bottom wall for v = 8 m/s

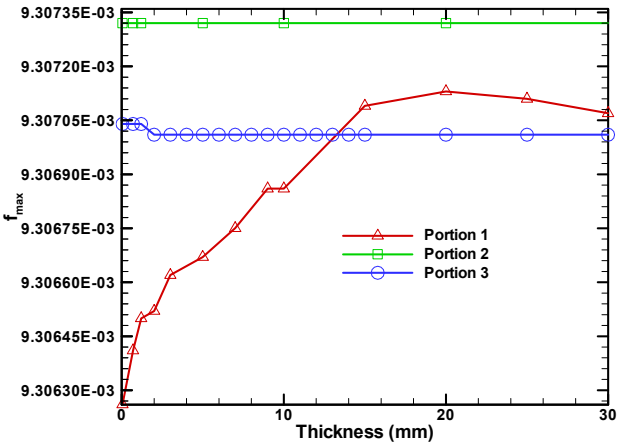

Fig. 3 (c) Evolution of the maximum friction on the bottom wall for v = 9 m/s

From Figs. 3 (a)-(c) we observe the impact of the velocity on the viscous friction, and therefore on the turbulent boundary layer near the walls in the first portion. Likewise, this portion is characterized by a strong variation in the coefficient of friction over a height of approximately 30 mm from the wall. The value of the maximum coefficient of friction is observed in this portion at ≈ 20 mm from the wall, for each speed considered. However, the maximum friction is observed in the second portion at all the speeds considered. Although constant, it drops with speed. Work is in progress to verify if the geographical arrangement of this portion is at the origin of this constant pace. This work is all the more justified by the shape of the friction observed in Section III.

Near the wall at a height of ≈ 2 mm, the maximum friction is observed in this portion. However, despite this small variation, it seems rather to have a constant pace. We observe that the friction also drops with speed.

Fig. 3 (a) also shows the impact of speed on turbulent friction. This is more visible in the third portion with variation in the shape of the turbulent friction, albeit slight.

B. Upper Wall

We start by presenting the evolution of the maximum friction f_{max} on the upper wall in the three portions considered, as a function of the thickness and for each considered speed.

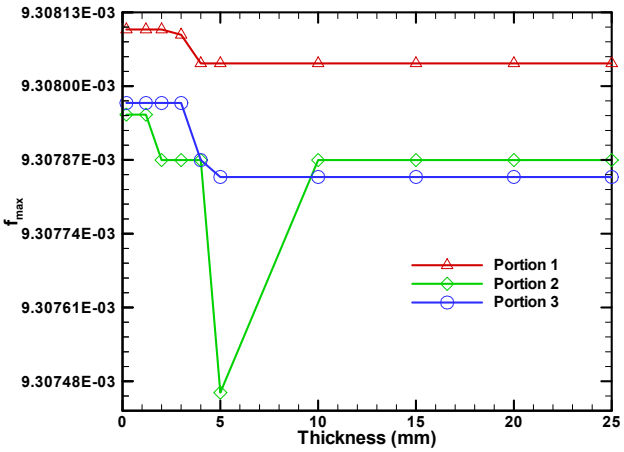

Fig. 4 (a) Evolution of the maximum friction on the upper wall for v = 7 m/s

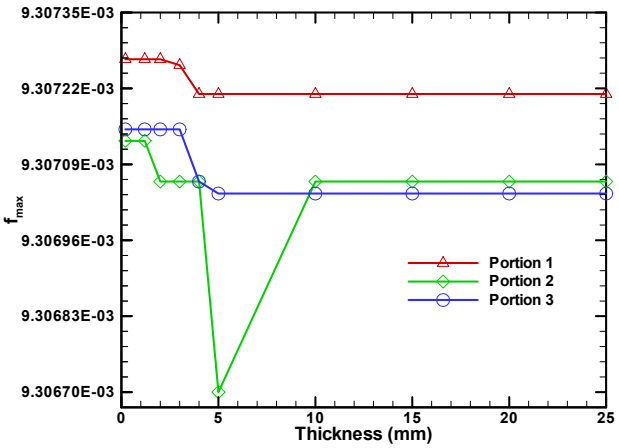

Fig. 4 (b) Evolution of the maximum friction on the upper wall for v = 8 m/s

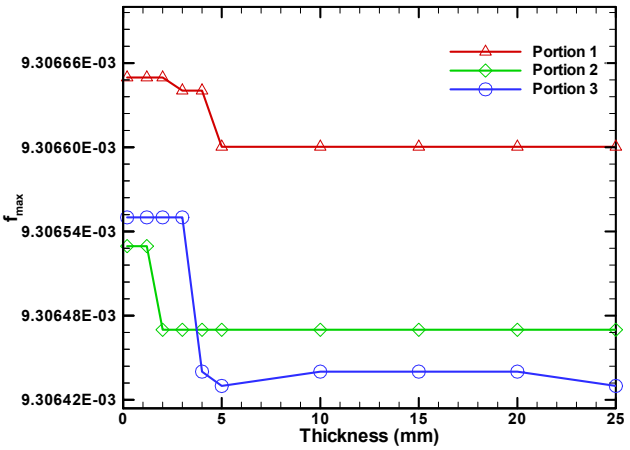

Fig. 4 (c) Evolution of the maximum friction on the upper wall for v = 9 m/s

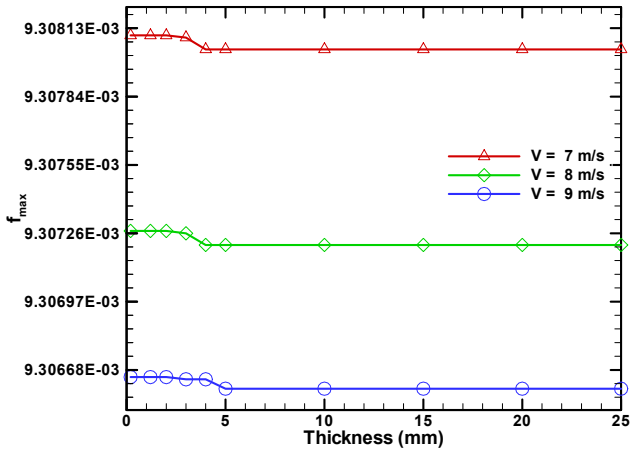

Fig. 5 (a) Evolution of the maximum friction on the upper wall in the portion 1

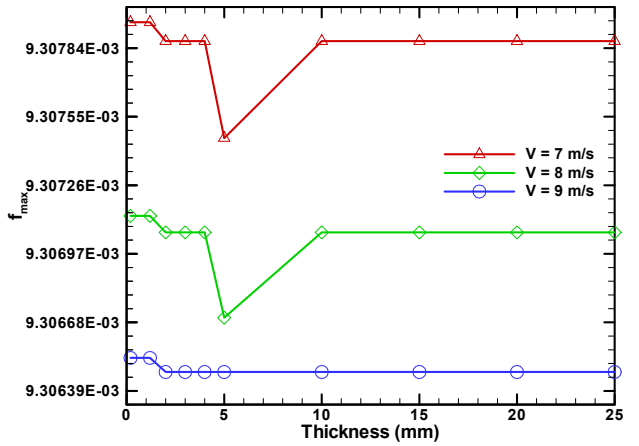

Fig. 5 (b) Evolution of the maximum friction on the upper wall in the portion 2

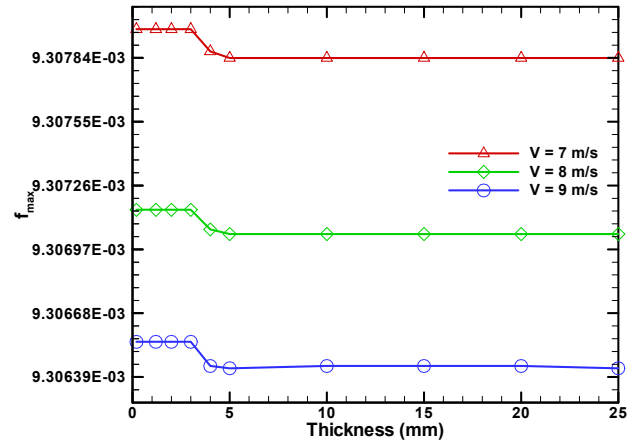

Fig. 5 (c) Evolution of the maximum friction on the upper wall in the portion 3

The maximum friction on this wall is found in the first portion for the three speeds considered. The thickness for a maximum coefficient of friction is ≤ 3 mm in all the portions, regardless of the speed considered. In the second portion, we observe a sharp drop in turbulent friction in the range 4 mm to 10 mm for speeds of 7 m/s and 8 m/s. We are still trying to understand this phenomenon. A slight variation is also observed in the third portion on the shape of the turbulent friction beyond 5 mm on this wall at a speed of 9 m/s. which is not the case for other speeds considered.

To observe the behavior of friction as a function of speed, we will subsequently group its evolution as a function of speeds for each portion.

The remark we can make of Figs. 5 (a)-(c) is the constant decrease in turbulent friction with speed. The gap may be smaller when heading towards high speeds and greater when heading towards low speeds.

C. Side Wall

Fig. 6 gives us the evolution of the maximum friction f_{max} on the side wall in the three portions as a function of the thickness.

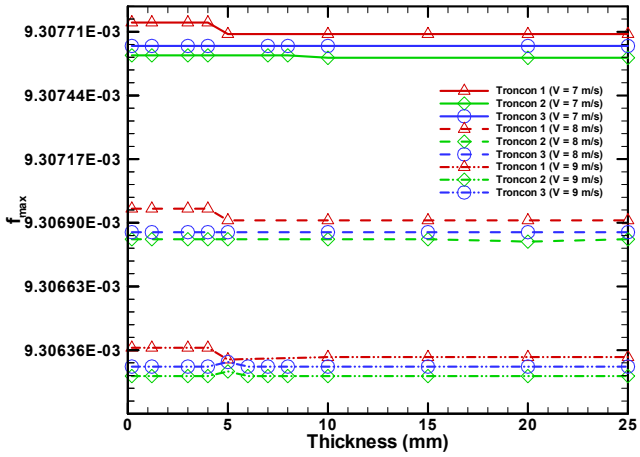

Fig. 6 Evolution of the maximum friction on the side wall

From Fig. 6, we observe that the evolution of turbulent friction is almost rectilinear. For each speed, the maximum friction is observed in the first portion with a height < 4 mm. This friction is lower in the second portion. It generally drops with speed as noted above.

Table I gives us a summary of the boundary layers for different speeds and in all portions.

TABLE I
THICKNESS FOR f_{max} VALUES

Walls	Portion	Thickness for f_{max}	Portion for f_{max}
Bottom	1	20	2
	2	0,05	
	3	0,05	
Upper	1	1,2	1
	2	1,2	
	3	1,2	
Side	1	4	1
	2	5	
	3	5	

The walls of this pipe do not have the same boundary layer because it varies in each portion. On the lower wall, the evolution of friction is much more curved for all portions. This

is consistent with the algebraic study giving a nonlinear character to the friction coefficients found by the formula proposed by Swamee and Jain. The angle of inclination of the pipe and the entry of the flow determine the evolution of friction. In the first portion, which represents the entrance to the penstock and whose grip is a compound surface, the friction gradually increases over about 20 mm of the wall. It then begins to decrease and subsequently becomes constant. In the other two portions, the friction is higher near the walls. It tends to become a constant as we move towards the penstock axis.

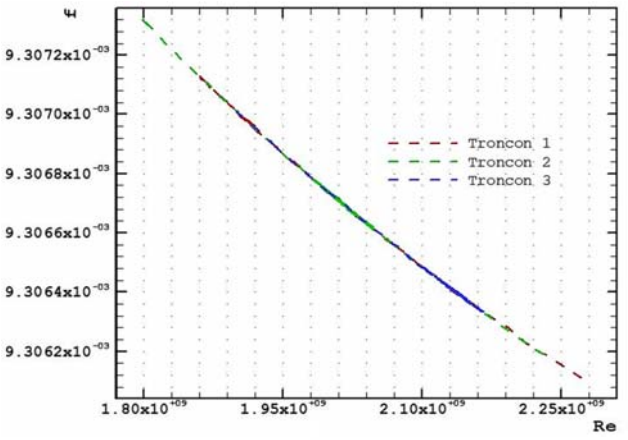

Fig. 7 (a) Evolution of the maximum friction on the bottom wall

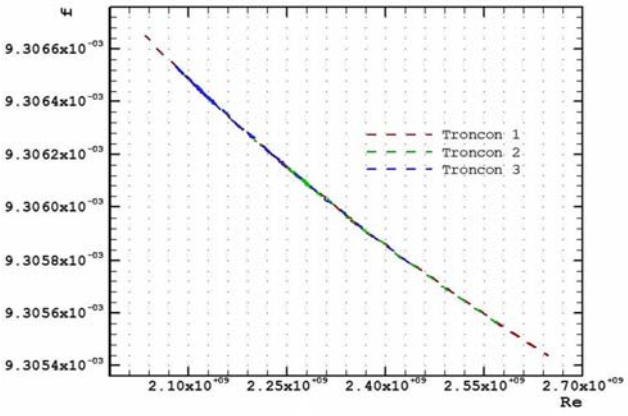

Fig. 7 (b) Evolution of the maximum friction on the upper wall

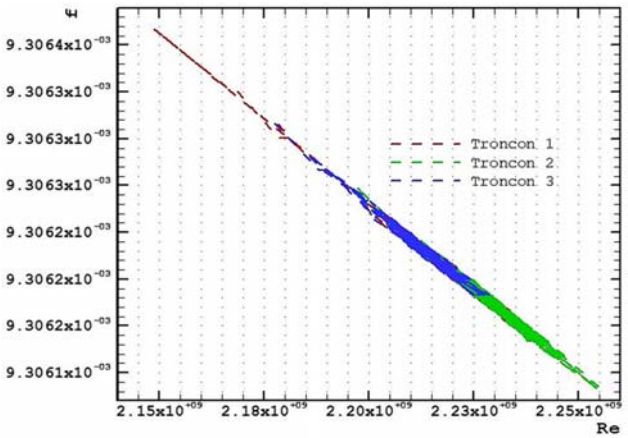

Fig. 7 (c) Evolution of the maximum friction on the side wall

The effect of speed on the turbulent friction in the three portions and for each wall can be summarized by Figs. 7 (a)-(c).

Then, the maximum friction in the second portion is observed on the bottom wall. It is rather maximum in the first portion on the top and side wall. However, it should be noted that it is difficult to obtain the exact value of the coefficient of friction as given algebraically. Indeed, Winning et al. [16] in the same logic as Swamee and Jain [4] proposed formulas allowing to directly calculate the value of the coefficient of friction in a pipe. We add to this list the method of Haaland [17], equations 2 and 3 of Serghides [18], or even more recently equations A and B of Brkić [19]; not forgetting one of the most used approaches which is that of Moody (determination from the Moody diagram) [20]. We therefore observe in these figures that the value of the coefficient of friction depends on several parameters which are difficult to obtain algebraically. On a theoretical basis, which is the basis on which most of the formulas and approaches used to determine the coefficient of friction are based, it emerges from all the figures that it varies in a portion of pipe. Likewise, it has unpredictable behavior on the side wall.

In reality, the formulas proposed by the above-mentioned researchers (and consequently the one commonly used) depend on constants such as the length of the pipe, its diameter, the relative roughness and the Reynolds number. These data are no less abstract, but also very far from the reality on the ground.

To compare our results, velocity profiles were drawn to observe the effects of turbulent friction on them. Figs. 8 and 9 therefore allow us to validate the model used to carry out this work.

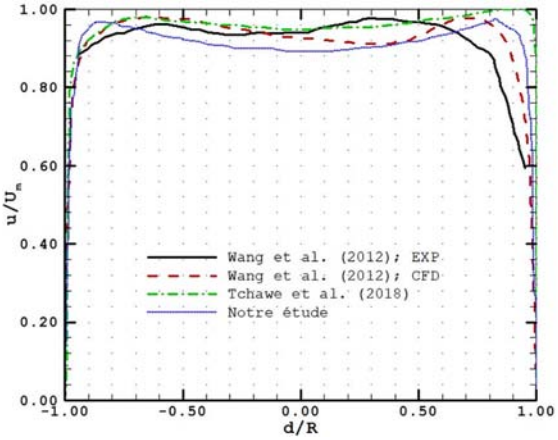

Fig. 8 Velocity distribution for our study, Wang et al. (EXP) [6], Wang et al. (CFD) [6] and Tchawe et al. [11]

We observe in Fig. 8 a concordance on the structure of the flow with the work of Wang et al. [6]. The comparison is more visible on the results obtained numerically in the light of these different works. This increasingly comforts researchers in the choice of this approach for solving engineering problems, because it makes it possible to visualize phenomena that are difficult to see or even impossible by the experimental approach. This is also one of the findings made by Abdalla et

al. [20] in their work on the detachment of the boundary layer upstream of a crossing threshold. Likewise, after several works on the subject, we have been reinforced by results obtained in this direction.

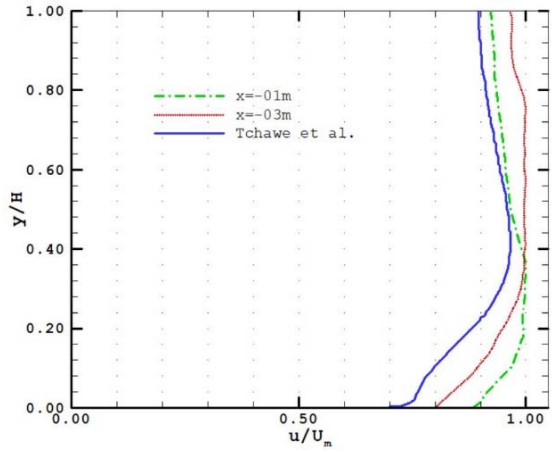

Fig. 9 (a) Velocity profile for our study and that of Tchawe et al. [7]-[11] upstream of the water intake

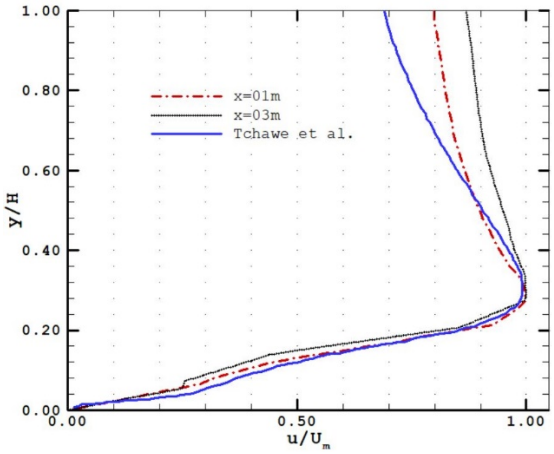

Fig. 9 (b) Velocity profile for our study and that of Tchawe et al. [7]-[11] in the intake

IV. Conclusion

In this work, we have numerically evaluated the friction on the walls of the penstock of the Three Gorges dam. We modeled the boundary conditions for the calculation of the flow under FLUENT. The calculations were made in 3D in order to take into account the wall effects. The formula used to calculate the friction is that proposed by Swamee and Jain, because it is widely used in the field of engineering. It turns out that depending on the wall, the friction changes differently. It is also difficult to obtain the exact value of the coefficient of friction as given algebraically, because it depends on several parameters which are difficult to obtain algebraically. As for the boundary layer, it varies according to the wall and according to the portion. However, it is more visible in the first portion of our penstock on a not insignificant height. Finally, we note that the numerical approach allows us to observe the effects on the walls better than with an experimental approach. It also makes it possible to describe the evolution of turbulent friction on the walls.

Acknowledgment

We sincerely acknowledge IUG-Cameroon which eased the realization of this work, and pay homage to its founder Louis-Marie DJAMBOU (rest in peace) who opened us the door to his institution.

References

[1] J. M. Chapallaz, H. P. Mombell, A. Renaud, J. C. Scheder & J. Graf, "Petites centrales hydrauliques : Turbines hydrauliques, Energies Renouvelables". PACER, ISBN 3-905232-54-5, N0 724.247.1f, 134 pages, (1995).

[2] C. F. Colebrook & C. M. White, "Experiments with Fluid Friction in Roughened Pipes". Proc. Roy. Soc., Series A, 161, 367, (1937).

[3] C. F. Colebrook, "Turbulent flow in pipes with particular reference to the transition region between the smooth and rough pipe laws". J Inst Civil Engineers, London, Vol. 11, pp. 133-156, (1939).

[4] P. K. Swamee, & A. K. Jain, "Explicit equations for pipe-flow problems". Journal of the Hydraulics Division. 102 (5): 657–664. (1976).

[5] B. Achour & A. Bedjaoui, "Calcul du coefficient de frottement en conduite circulaire sous pression". Larhyss Edition Capitale, ISSN 1112-3680, n0 05, pp. 197-200, (2006).

[6] C. Wang, T. Meng, H. Hu, L. Zhang, "Accuracy of the ultrasonic flow meter used in the hydroturbine intake penstock of the Three Gorges Power Station". Flow Measurement and Instrumentation, 25: 32–39. (2012), https://doi.org/10.1016/j.flowmeasinst.2011.12.003

[7] N. F. Nkontchou, T. M. Tchawe, N. M. Tientcheu, T. Djiako, B. Djeumako, D. Tcheukam-Toko, Determination of the Dynamic Field in the Penstock of the Trois-Gorges Dam by a Numerical Approach, International Journal of Energy Engineering, Vol. 11 No. 1, pp. 9-16. 2021. https://doi.org/10.5923/j.ijee.20211101.02.

[8] T. Von Karman, "The fundamentals of the statistical theory of turbulence". Journal of Aeronautical Science, 4, 131-138, (1934).

[9] D. Wilson, Turbulence modeling for CFD. DCV industries, 2nd Edition, 1998.

[10] T. M. Tchawe, B. Djeumako, C. Koueni-Toko, D. Tcheukam-Toko & A. Kuitche, "Study of Dynamic Field around a Vertical Circular Cylinder placed in an Open-Chanel Flow". International Journal of Innovative Science, Engineering & Technology, Vol. 2, pp.6. (2015).

[11] T. Tchawe, D. Tcheukam-Toko, B. Kenmeugne, T. Djiako, "Numerical study of flow in the water inlet of the penstock of a hydroelectric dam", International Journal of Current Research, 10, (7), 71061-71066. https://doi.org/10.24941/ijcr.31203.07.2018

[12] Prandtl, "Ergebnisse Göttingen". 1932, 4, p.

[13] Boussinesq, "Théorie de l'écoulement tourbillonnant et tulmultueux des liquides". Paris, 1897.

[14] Fluent, User manual 6.3.26. (2006).

[15] W. Zhang, J. Yuan, J. Han, C. Huang and M. Li, "Impact of the Three Gorges Dam on sediment deposition and erosion in the middle Yangtze River: a case study of the Shashi Reach". Hydrol. Res. 47 (S1), 175–186. (2016)

[16] S. Haaland, "Simple and Explicit Formulas for the Friction Factor in Turbulent Pipe Flow". Journal Fluids Engineering, 105, 89-90, (1983). DOI: 10.1115/1.3240948

[17] T. K. Serghides, "Estimate friction factor accurately". Chem. Eng. 91(5), 63–64, 1984.

[18] D. Brkić. "Review of explicit approximations to the Colebrook relation for flow friction". Journal of Petroleum Science and Engineering, Elsevier, 2011, 77 (1), pp.34-48. 10.1016/j.petrol.2011.02.006.

[19] L. F. Moody, "Friction Factors for Pipe Flow", Transactions of the ASME. 66 (8): 671–684, (1944).

[20] I. Abdalla, Y. Zhiyin & C. Malcolm, "Computational analysis and flow structure of a transitional separated-reattached flow over a surface mounted obstacle and a forward-facing step." International Journal of Computational Fluid Dynamics, Vol. 23, No. 1, 25–57, January 2009.